Spatial and temporal distribution of precipitation in a Mediterranean area (southern Italy)

A. Longobardi [1], G. Buttafuoco [2*], T. Caloiero[2] and R. Coscarelli[3]

(1) Department of Civil Engineering, University of Salerno, 84084 Fisciano (SA), Italy

(2) National Research Council of Italy – Institute for Agricultural and Forest Systems in the Mediterranean (CNR-ISAFOM), 87036 Rende (CS), Italy

(3) National Research Council of Italy – Research Institute for Geo-Hydrological Protection (CNR-IRPI), 87036 Rende (CS), Italy

[*] Corresponding author. Via Cavour 4/6, 87036 Rende (CS) Italy. Tel. +39 0984 841484; e-mail address: gabriele.buttafuoco@cnr.it

"This is a post-peer-review, pre-copyedit version of an article published in Environmental Earth Sciences. The final authenticated version is available online at:http://dx.doi.org/10.1007/s12665-015-5045-8"

Abstract. The precipitation climate regime of a region is characterized by the distribution of the monthly precipitation contribution. Its temporal and spatial analysis is particularly interesting for many fields of applied sciences, such as climatology, hydrology and water resources management. With the aim to describe the climate regime, its spatial feature and relevant potential temporal shift, for a large area of southern Italy (Mediterranean basin), a database of about 559 stations has been explored through the statistical analysis of rainfall time series spanning between 1917 and 2006. After a change point analysis, aimed at the assessment of data quality, a trend analysis has been performed on both monthly precipitation, monthly percentage of annual rainfall amount and PCI-computed series. The broad extension of the area under investigation highlights a better understanding of precipitation distribution patterns over space. Results of PCI trend analysis show a significant shift, for about 40–50 % of total gauging station, over the time towards a more uniform climate regime, especially for

the hilly areas. Moreover, the trend analysis on the monthly rainfall series indicates that the shift is produced by a reduction of rainfall amount during the winter season, particular consistent over the Tyrrhenian side of the peninsula, and an increase during the summer season quite widespread over the whole investigated territory.

Keywords: Precipitation, PCI, climate regime, trend, Mediterranean basin.

Introduction

During the past century, with growing concerns about the impacts of climatic changes, precipitation trend analysis, on different spatial and temporal scales, has been one of the most extensively research and debated issue. The fifth IPCC Assessment Report (AR5) confirmed an increase in the Earth's surface temperature in the twentieth century and forecasted a further increase for the twenty-first century (IPCC 2013). Moreover, droughts will intensify in the twenty-first century in some seasons and areas, following reduced precipitation and/or increased evapotranspiration. This phenomenon will concern regions such as southern Europe and the Mediterranean region, central Europe, central North America, Central America and Mexico, northeast Brazil, China, Oceania and southern Africa (IPCC 2013). The magnitude and the effect of these changes have been recently analysed by several researchers (De Luis et al. 2000; Xoplaki et al. 2006; Feidas et al. 2007; Zhu and Meng 2010; del Rio et al. 2011, Martins et al. 2012; Dashtpagerdi et al. 2015; Shi et al. 2014; Caloiero 2015; Feng and Zhao 2015; Kundu et al. 2015; Lu et al. 2015; Wei et al. 2015).

With reference to the southern regions of Europe (the Mediterranean basin), the AR5 stressed how these areas appear particularly vulnerable to potential future alternations of extreme rainy periods and droughts or scarcity of water resources. Furthermore, the Mediterranean basin is characterized by a large precipitation variability at regional scale (Mehta and Yang 2008; Reale and Lionello 2013) which is related to synoptic dynamics of hazardous events moving and evolving along the Mediterranean basin (Lionello and Giorgi 2007).

Several studies involving Italian long-term precipitation databases showed a strong reduction in precipitation over the last 50 years (Palmieri et al. 1991; Brunetti et al. 2004, 2006; Sirangelo et al. 2015). More detailed analyses presented negative trends at regional level, as in Southern Italian regions such as: Campania (Diodato 2007, Longobardi and Villani 2010), Basilicata (Piccarreta et al. 2004) and Calabria (Coscarelli et al. 2004;Caloiero et al. 2011a, b; Brunetti et al. 2012). The same studies confirmed that these trends behave differently depending on their time of observation throughout the year: a tendency towards a reduction of precipitation amount during the winter months and an increase during the summer months have been detected.

Precipitation distribution during the year, which characterizes the climate regime of a given area, is a very important issue in climatology studies. A rather unbalanced precipitation distribution determines the presence of seasons with an excess of precipitation and seasons where, instead, a deficit occurs, with obvious implications for water resources management. A conventional system for quantifying the distribution of precipitation during the year is given by the introduction of the Precipitation Concentration Index (Oliver 1980), whose computation can be performed when precipitation data, aggregated at monthly scale, are available. The Precipitation Concentration Index (PCI), by definition, characterizes climate regimes, but it can also be used to detect changes in climate regimes over time, as a result of climate variability. PCI has been used by several authors in the Mediterranean areas (Michiels et al. 1992; Apaydin et al. 2006; Raziei et al. 2008; De Luis et al. 2011; Martins et al. 2012) and in the rest of the world (Singh et al. 1989; Xu et al. 2010; Ngongondo et al. 2011; Elagib 2011; Nsubuga et al. 2014; Shi et al. 2014). By contrast, very few applications concerning the Italian territory are available and they all focus on the single southern regions (Cannarozzo et al. 2006; Longobardi et al. 2011; Coscarelli and Caloiero 2012). In particular, Cannarozzo et al. (2006), by applying the Mann–Kendall test to the PCI values of the Sicily region territory, a general steady situation emerged in which the rainfall temporal distribution during the year has not been modified. In the Campania region, Longobardi et al. (2011) detected a moderate-to pronounced seasonality in the precipitation regime, with a negative PCI trend during the last century. This trend indicated a tendency of the precipitation distribution throughout the year moving towards a more uniform pattern. Similar results have also been obtained for the Calabria region (Coscarelli and Caloiero 2012).The main contribution of this study is represented by the spatial scale of observation because, unlike other previous studies, which focused on small study areas, this paper highlights how analysing a wider area can offer a better understanding of precipitation distribution patterns over space, behind time. The broad spatial extension of the analysis has entailed a merging procedure of several monthly precipitation databases, which provided data for 559 rain gauges with observations spanning from 1917 to 2006, preliminary tested for quality control and to set up a homogeneous database.

With the aim to describe the climate regime, its spatial feature and relevant potential temporal shift, the following analyses have been performed: (1) the spatial and temporal pattern of monthly precipitation; (2) the spatial and temporal precipitation seasonality by means of an index-based PCI approach; (3) the spatial and temporal monthly percentage of annual rainfall amount.

Material and methods

The study area

The region under investigation is a large portion of the Italian peninsula, extending from the Campania and the Apulia regions in the North, to Sicily in the South, and covering an area of about 85,000 km^2 (Figure 1). It is located within the Mediterranean basin and due to the difference in the latitudes within which the study area extends, climatic conditions have markedly different elements. Figure 2 shows the mean annual precipitation map for the study area. Larger precipitation are recorded near the tallest reliefs, because of the significant orographic effect on precipitation. Yearly precipitation reaches maximum values of about 2,000 mm in the Campania region and minimum values of about 400 mm in Sicily. The climate regime of the study area is typically seasonal with some evident differences depending on the location of the station. The box in Figure 2 shows the mean monthly precipitation proportional coefficients (ratio between mean monthly and annual precipitation) for each region of the study area where the “Mediterranean” and the “Apennine” regimes prevail. In the Mediterranean climate, which dominates almost all the study area, and in particular the islands and the coastal areas, the winter season is a rather mild and rainy period, whereas the summer season is very hot and dry. In the Apennine climate, dominating the inland and the mountainous areas, winter and summer are very cold and hot seasons respectively, and precipitation is rather uniformly distributed throughout the year.

Available data and change point analysis methods

Available data consist of monthly precipitation registrations of 891 meteorological stations, over a long-term period, spanning from 1917 to 2006. Most long-term climatic series are affected by non-climatic factors indeed: changes in instruments, station location, station environment and so on make climate data unrepresentative of temporal climate variability. Non homogeneities produce either sharp discontinuities or gradual bias in the data, which can be detected with the use of statistical tests. A large number of approaches for change point detection have been indeed proposed and when applied to the same series, they could actually yield conflicting conclusions, because of different climate elements relevant to the time series under investigation (Reeves et al., 2007). Given to this reason, it could be advisable to apply a number of regime shift detection methods and further critically compare them.

In the current paper, interest is in particular devoted to the detection of shift in the mean of the process and to this aim two different approaches have been considered. These are: i) the cumulative CUMSUM test (Efron and Tibshirani, 1993and ii) the non-parametric Mann–Whitney test (Pettitt, 1979).

The CUMSUM test is a cumulative test which statistic S is defined as:

$$S_t=S_{(t-1)}+(x_t-\mu) \qquad t=1\ldots..T \qquad (1)$$

where T is the sample length and μ is the sample mean. The series is homogeneous if S is approximately 0. If St shows a maximum (minimum) a negative (positive) shift would be detected. The significance of the shift can be evaluated calculating the 'rescaled adjusted range' variable:

$$R=(\max S_t-\min S_t)/\sigma_x \qquad (2)$$

where σ_X is the time series standard deviation. Critical values for R are given in Buishand (1982).

The Pettitt's test is a nonparametric test, that requires then no assumption about the distribution of data. It tests the H_0: the T variables follow one or more distributions that have the same location parameter (no change), against the alternative Ha: a change point exists. If T is the length of the time series, xt = {x1, x2, …., xt} and xj = {xt+1, xt+2, …., xT}, the non-parametric statistic is defined as:

$$K_T = max|U_{t,T}| \qquad (3)$$

where

$$U_{t,T} = \sum_{i=1}^{t} \sum_{j=1}^{T} sgn(x_t - x_j) \quad (4)$$

The change-point of the series is located at K_T, provided that the statistic is significant. For the change point, the probability of occurrences is:

$$p(t) = 1 - exp\left(\frac{-6U_{t,T}^2}{T^3+T^2}\right) \quad (5)$$

The described tests have been applied to detect non homogeneities within long-term yearly precipitation data set of the 891 rain gauge stations, over the period from 1917 to 2006, for a significance level α = 5%. As periodicity and autocorrelation in observed data could affect the analysis of the test results, the change point detection procedure is here applied with reference to annual rainfall time series (Reeves et al., 2007). The two different approaches, applied to a particular time series, have provided contrasting results. As a general rules, it has been decided to critically compare the results of the tests and to conceptually intersect them. Then it has been assumed that a time series can be defined non homogeneous if both method detected a change point occurring at the same year. At the end of the quality control procedure, 559 (overall about 37% of total stations, rather uniformly distributed over the regions) out of the 891 monthly precipitation series emerged as homogeneous in the period 1917–2006 and thus suitable for long term analysis, while 332 series were discarded (Figure 1). The average density of the final database is 1 station per 138 km^2, with an average of 67 years of observations.

Trend detection analysis methods

Time series of monthly rainfall, for homogeneous rain gauge stations, have been tested for linear trend detection in time. A trend is a significant change over time exhibited by a random variable, detectable by statistical parametric and non-parametric procedures. In particular, the current study have provided and compared results for non-parametric Mann Kendall and Sen's tests approaches. Brief detail of the procedure are given below.

The MK test is a rank-based method for evaluating the presence of trends in time-series data, without specifying whether the trend is linear or non-linear. The data are ranked according to time, and then each data point is compared to all the data points that follow in time. The MK statistic (Kendall 1962) is given by:

$$S = \sum_{i=1}^{n-1} \sum_{j=i+1}^{n} \operatorname{sgn}\left(x_j - x_i\right) \tag{6}$$

where x are the data value at times i and j, n is the length of the data set and *sgn(z)* is equal to +1, 0, -1 if z is greater than, equal to, or less than zero respectively. Under the null hypothesis that x_i are independent and randomly order, for n greater than 8, the statistic S is approximately normally distributed with zero mean and variance:

$$Var(S) = \left[n\left(n-1\right)\left(2n+5\right) - \sum_{i=1}^{n} t_i \; i \; \left(i-1\right)\left(2i+5\right) \right] \Big/ 18 \tag{7}$$

where t_i denotes the number of tied values of extent i.

The standardized test statistic Z, computed by:

$$Z_{MK} = \begin{cases} \dfrac{S-1}{\sqrt{Var(S)}} & \text{for } S > 0 \\ 0 & \text{for } S = 0 \\ \dfrac{S+1}{\sqrt{Var(S)}} & \text{for } S < 0 \end{cases} \tag{8}$$

follows a standard normal distribution (Kendall 1962).

The probability value, p, of the Z_{MK} statistic of sample data can be estimated by using the normal cdf $\Phi(Z_{MK})$:

$$p = 1 - \Phi\left(Z_{MK}\right) = 1 - \frac{1}{\sqrt{2\pi}} \int_0^{Z_{MK}} e^{-t^2/2}\, dt \tag{9}$$

At the significance level α, the existing trend is considered to be statistically significant if $p \leq \alpha/2$ in the case of the two-tailed test (Caloiero et al. 2011b).

Sen (1968) developed the non-parametric procedure for estimating the slope of trend in the sample of N pairs of data:

$$Q_i = \frac{x_j - x_k}{j - k} \quad for\ i = 1, \ldots, N \tag{10}$$

where x_j and x_k are the data values at times j and k (j>k), respectively.

If there is only one datum in each time period, then $N = n(n-1)/2$ where n is the number of time periods. If there are multiple observations in one or more time periods, then $N = n(n-1)/2$ where n is the total number of observations.

The N values of Q_i are ranked from smallest to largest and the median of slope or Sen's slope estimator is computed as:

$$Q_{med} = \begin{cases} Q_{[(N+1)/2]} & \text{if } n \text{ is odd} \\ \dfrac{Q_{[N/2]} + Q_{[(N+2)/2]}}{2} & \text{if } N \text{ is even} \end{cases} \tag{11}$$

The Q_{med} sign reflects data trend reflection, while its value indicates the steepness of the trend.

Precipitation Concentration Index

Climate seasonality has been quantified, at each point station, through the calculation of the PCI index, first introduced by Oliver (1980) and then modified by De Luis (2011), as follows:

$$PCI_j = 100 \frac{\sum_{i=1}^{12} P_{ij}^{\,2}}{\left(\sum_{i=1}^{12} P_{ij} \right)^2} \tag{12}$$

where P_{ij} is the amount of rainfall for the *i*-th month and the *j*-th year and PCI_j is the Precipitation Concentration Index for a particular year j. The long-term average *PCI*, considered in the following analysis, would be:

$$PCI = \frac{1}{N}\sum_{j=1}^{N} PCI_j \qquad (13)$$

where *N* is the number of years of observations. According to Oliver (1980), values below 10 indicate a uniform precipitation distribution, values from 11 to 20 denote seasonality in precipitation distribution, and values above 20 correspond to climates with substantial monthly precipitation variability.

Firstly, the average long term PCI data (see equation 13) have been spatially predicted and mapped to represent the climate regime distribution over the investigated region. This section is more extensively described in the following section. Secondly, in order to investigate the temporal effect of the changing precipitation distribution throughout the year, the PCI time series (see equation 12) have been tested for linear trend detection, with the application of the same trend detection tests used for monthly precipitation analysis.

Geostatistical methods

To characterize the long-term climate regime of the study area, the long-term average *PCI* data were predict in a spatial sense from punctual data and mapped using a geostatistical approach (Webster and Oliver 2007). *PCI* data were modelled as an intrinsic stationary process and each *PCI* datum $z(\mathbf{x}_\alpha)$ at different location $\mathbf{x}_\alpha$ ($\mathbf{x}$ is the location coordinates vector and α the sampling points = 1, ..., N) was interpreted as a particular realization of a random variable $Z(\mathbf{x}_\alpha)$. The set of random variables $Z(\mathbf{x}_1)$, $Z(\mathbf{x}_2)$, ..., for all $\mathbf{x}_\alpha$ in the study area constitutes a random function. The set of actual values of Z compring the realization of the random function is known as a regionalized variable $z(\mathbf{x}_\alpha)$. Interested readers should refer to textbooks such as Goovaerts (1997), Chilès and Delfiner (2012), Wackernagel (2003), Webster and Oliver (2007), among others, for a detailed presentation of the theory of regionalized variables. An objective of geostatistics is to quantify and exploit spatial pattern of regionalized variables. The most common measure of spatial correlation of the regionalized variable $z(\mathbf{x}_\alpha)$ is the experimental variogram $\gamma(\mathbf{h})$ (Webster and Oliver 2007):

$$\gamma(\mathbf{h}) = \frac{1}{2N(\mathbf{h})} \sum_{\alpha=1}^{N(\mathbf{h})} \left[z(\mathbf{x}_\alpha) - z(\mathbf{x}_\alpha + \mathbf{h}) \right]^2 \tag{14}$$

where $N(\mathbf{h})$ is the number of data pairs for a given class of distance and direction. The experimental variogram $\gamma(\mathbf{h})$ is a function of the distance vector ($\mathbf{h}$) of data pairs values $[z(\mathbf{x}_\alpha), z(\mathbf{x}_\alpha + \mathbf{h})]$. A theoretical function, called variogram model, is fitted to the experimental variogram and allows the analytical estimate of the variogram for any distance $\mathbf{h}$. The variogram model generally requires two parameters: range and sill. The range is the distance over which pairs of *PCI* values are spatially correlated, while the sill is the variogram value corresponding to the range. The optimal fitting is chosen on the basis of a cross-validation test, which checks the compatibility between the data and the structural model considering each data point in turn, removing it temporarily from the data set and using its neighbouring information to predict the value of the variable at its location. The estimate is compared with the measured value by calculating the experimental error, i.e. the difference between them, which can also be standardized by estimating the standard deviation. The goodness of fit was evaluated by the Mean Error

(*ME*) and the Mean Squared Deviation Ratio (*MSDR*). The mean error (*ME*) proves the unbiasedness of estimate if its value is close to 0:

$$ME = \frac{1}{N}\sum_{\alpha=1}^{N}\left[z^*(\mathbf{x}_\alpha) - z(\mathbf{x}_\alpha)\right] \quad (15)$$

where N is the number of observation points, $z^*(\mathbf{x}_\alpha)$ is the predicted value at location α, and $z(\mathbf{x}_\alpha)$ is the observed value at location α. The mean squared deviation ratio (*MSDR*) is the ratio between the squared errors and the kriging variance ($\sigma^2(\mathbf{x}_\alpha)$) (Webster and Oliver, 2007):

$$MSDR = \frac{1}{N}\sum_{\alpha=1}^{N}\frac{[z^*(\mathbf{x}_\alpha) - z(\mathbf{x}_\alpha)]^2}{\sigma^2(\mathbf{x}_\alpha)} \quad (16)$$

where N is the number of observation points, $z^*(\mathbf{x}_\alpha)$ is the estimated value at location α, and $z(\mathbf{x}_\alpha)$ is the observed value at location α. If the model for the variogram is accurate, the mean squared deviation ratio should approximate kriging variance and *MSDR* value should be close to 1.

The fitted variogram was used to estimate *PCI* values at ungauged locations using ordinary kriging (Webster and Oliver 2007) at the nodes of a 250 m x 250 m interpolation grid. All statistical and geostatistical analyses were performed by using the software package ISATIS®, release 2014.1 (www.geovariances.com).

Results and discussion

Trend analysis of monthly precipitation

The results of the trend analysis applied to the monthly precipitation, for each region and for the whole investigated territory, are summarized in Figures 3-5 with different statistical significance level (SL) (0.10; 0.05; 0.01). Trend detection significance is further spatially represented in Fig. 6. The months featured by diffused negative trend are January, November, February and December. In particular, considering the whole territory, 41.5% of the rain gauges present a negative significant trend (SL=0.10) with a maximum value in Campania region (about 60% of the rain gauge), (Fig. 3). Obviously, these percentages decrease considering lower SLs. As an example, with a SL equal to 0.01, only 9% of the whole rain gauge network presents a negative significant trend in January (Fig 3f).

From a spatial point of view (Fig. 6), the precipitation decrease in January has been detected in the entire study area, with more statistically significant values in the Tyrrhenian side of Calabria and Sicily (darker triangles), while in Campania and northern Basilicata opposite trend signs have been evaluated in the same period. A negative trend has also been observed in the Mediterranean side of Sicily and in the south-eastern area of the Apulia region (Fig. 6). Similar results, but with less significant values, have been observed in February, while in December a clear spatial distribution trend cannot be observed; a marked negative trend has been only detected in Calabria (Fig. 6).

A negative trend has also been detected in the spring months (Figs. 3, 4, 5), mainly in March. In particular, considering a SL of 0.10, a negative behaviour has been detected for 23.9 % of the whole network (Fig. 3f) with a maximum value of 50 % for the Sicily region (Fig. 3e). Geographically, this behaviour mainly concerns the Mediterranean and the Tyrrhenian sides of Sicily, the southern area of Calabria and the northern area of

Campania (Fig. 6). In April, an opposite trend has been observed (Figs. 3, 4, 5): 15.5 % of the whole network (Fig. 3f) presents a significant positive trend (SL = 0.10), in particular (Fig. 3e) for Sicily (25 % of the rain gauge). These positive values are detected in the Tyrrhenian side of the study area, in the Mediterranean side of Sicily, in the south-eastern area of Apulia and in the inland areas between Campania, Apulia and Basilicata (Fig. 6). In May, different regional trends have been mainly detected with more diffused negative values in Basilicata, Campania and Calabria, while positive values are more diffused in Apulia and western Sicily (Figs. 3, 4, 5, 6).

Conversely, summer precipitation shows a positive trend. In particular, in August 45.4 % of the whole rain gauge network (Fig. 3f) showed a significant positive trend (SL = 0.10), especially in Basilicata (69 %, Fig. 3a) and Campania (52.3 %, Fig. 3c). Also in July a spatially diffused positive trend has been evidenced in 36.0 % (SL = 0.10) of the whole territory (Fig. 3f) with a maximum percentage (Fig. 3d) value in Apulia 51 %. Conversely, in June 24.1 % (SL = 0.10) of the total rain gauges (Fig. 3f) present a negative tendency, especially observed in Basilicata, Calabria and Campania (Figs. 3, 4, 5, 6).

In the autumn months, a positive trend has been observed in almost all the study area (Fig. 3f) in September (17.4 % with a SL of 0.10) while a negative trend has been detected in November, in particular in Sicily, on the Ionian side of Calabria and Basilicata and in the south-eastern area of Apulia (Figs. 3, 4, 5, 6).

These findings, resulted from the analysis of a dense and homogeneous database, covering the entire southern Italy and with a dense database, confirmed a tendency towards a reduction in the precipitation amount during the winter months and an increase during the summer months which has been detected in various regional studies (Diodato

2007; Longobardi and Villani 2010; Buttafuoco et al. 2011; Caloiero et al. 2011a, b, 2015; Brunetti et al. 2012; Ferrari et al. 2013; Piccarreta et al. 2013). Figure 7 shows the results of the trends magnitude quantified by using the Sen's slope estimators. In January the trend showed the highest negative values particularly in Calabria (-47 mm/10 years) and in Campania (-32 mm/ 10 years). High negative values of trend were also evidenced in February (-34 mm/10 years) and in November (-29 mm/10 years). The positive trend magnitude is instead rather moderate: the largest positive rate is equal to 17.3 mm/10 years in Campania.

Spatial distribution and trend of the Precipitation Concentration Index

A variographic analysis was carried out to quantify the spatial pattern of the long-term average PCI data and a variogram map (not shown) was calculated to detect differences of spatial continuity with direction (anisotropy). The variogram map showed an anisotropic behaviour for PCI data. The direction of maximum continuity was north–south, whereas the one of minimum continuity was along the east–west direction. Subsequently, the experimental variogram (Eq. 14) was computed and a zonal anisotropy (box in Fig. 8) was evident from the differences in sill in the two directions (N–S and E–W). The anisotropic variogram shows greater variability in the north–south direction.

Moreover, the box in Fig. 8 shows that the more the distance between observations increases, the slower the variability in the N–S direction than in the E–W one. Therefore, a nested directional variogram model was used including three basic structures (Table 1): (1) a nugget effect (sill 0.2089); (2) a spherical model (Webster and Oliver 2007) along the N–S direction (range about 285 km; sill 3.6608); (3) a spherical model along the E–W direction (range about 77 km; sill 1.5382). The nugget effect is a discontinuity at the origin of the variogram and relates to measurement errors and to spatial sources of variations at smaller distances than shorter sampling intervals (Journel and Huijbregts 1978).

The goodness of fitting for the variogram model was verified by cross-validation and the results were quite satisfactory because the statistics used, i.e., mean of the estimation error and the mean squared deviation ratio, were quite close to 0 and 1, respectively.

Finally, the fitted variogram model was used with ordinary kriging to spatially predict and map (Fig. 8) the values of long-term average PCI. Results revealed that the index mostly ranges from values greater than 10 to values above 20, that is, precipitation distribution varies from almost uniform to strongly seasonal features (Fig. 8). There is a spatial increase in long-term average PCI moving from northern to southern latitudes. The lowest values correspond to the Apennine areas of Campania and Basilicata

regions, where the precipitation distribution is rather uniform, and the summer contribution to the yearly precipitation is not completely negligible. By contrast, the highest values occur in eastern Calabria and south-eastern Sicily, which are well known for their droughty summers and show a particularly marked climate seasonality. However, the broader extension of the territory is represented by a moderate climate seasonality with long-term average PCI values ranging between 12 and 15 as for what concerns the typical Mediterranean climate.

To investigate the temporal variability of the PCI, the MK test has been applied, for each rain gauge, to the PCI time series (see Eq. 12), detecting potential trends and their signs, at different significance levels (0.10, 0.05, 0.01). Figure 9 shows the results of the application of the trend analysis for each region and for each SL. The spatial distribution of the trend has been reported in Fig. 10. The histograms (Fig. 9) clearly show a negative trend affecting the largest fraction of the total database, about 40 % of the whole rain gauge network (Fig. 9f) with a SL = 0.10. This percentage reaches a maximum value (more than 50 % of the rain gauges) in Calabria (Fig. 9b). The spatial distribution of the negative trends is also evident in Fig. 10a. More findings are provided by the assessment of the trend magnitude, estimated through the Sen’s slope. In particular, negative values (Fig. 10b) have been mainly found in Calabria (where the largest negative magnitude is about -0.6/10 years), on the Tyrrhenian and western-Mediterranean sides of Sicily, in the south-eastern area of Apulia and in the inland areas between Campania, Apulia and Basilicata.

These results show a tendency towards a more uniform distribution of the monthly precipitation during the year, which would be a benefit for those regions (typically the Mediterranean basin) stressed, especially during the summer season, by an increase in water demand and a reduction in available water resources. Reported finding confirms the tendencies detected by the application of the MK test to the monthly precipitation series, providing, however, a more rapid and synthetic interpretation of the results.

Trend analysis of the monthly percentages of the annual rainfall amount

As a result of the trend analysis on the monthly precipitation of the study area, a reduction in precipitation amount during the winter months and an increase during the summer months have been identified. As previously evidenced, these results are relevant for areas such as southern Italy, where water resources management is particularly affected by the local climate conditions. To quantify the precipitation distribution during the year, the monthly percentages of the annual amount precipitation have been evaluated. The results of the application of the trend analysis (at various statistical significance levels: 0.10, 0.05, 0.01) are shown in Figs. 11, 12, 13. The most important result is an increase in the summer precipitation contribution in particular in August (53.4 % of the all rain gauges—SL = 0.10) and July (40.3 %). This trend is mainly evidenced (82.8 % of the regional rain gauges) in the Basilicata region (Fig. 11a). A positive behaviour has also been detected in spring and autumn (Fig. 11f), in particular in April (27.2 %) and September (32.3 %). On the contrary, a negative trend (Fig. 11f) has been detected in January (20.2 %), June (18.4) and November (12.7 %). The percentages obviously decrease in absolute value considering lower values of SLs (Figs. 12, 13).

As to what concerns the distribution of the trends in the winter period, a general decrease has been detected only in January, with significant values in the Tyrrhenian side of the study area, in particular in Calabria, western Sicily and partially in Campania (Fig. 14). In spring, and especially in April, the opposite trend has been observed, with positive values registered on the Tyrrhenian side of the study area, on the western Mediterranean side of Sicily, in the southern eastern area of Apulia and in the inland areas between Campania, Apulia and Basilicata (Fig. 14). The strongest positive trend has been evaluated during the summer season and this trend affected the whole study area in July and above all in August (Fig. 14). In June, a negative trend has been identified in Calabria and Sicily, while the opposite trend has been detected in Apulia (Fig. 14). Finally, in autumn, while a positive trend has been observed in September, in particular in Calabria and Sicily (Fig. 14), a negative trend has been detected in November and especially on the Ionian side of Calabria (Fig. 14).

Conclusions

The main purpose of this paper has been the analysis of the spatial and temporal patterns of the climate regime for a large area in Southern Italy, in a typical Mediterranean region. Unlike previous studies, which focused on small study areas, the present paper highlights how the study of a wider area can offer a better understanding of precipitation distribution patterns over space, behind time. The broad spatial extension of the analysis has entailed a merging procedure of several monthly precipitation databases, which provided data for 559 homogeneous rainfall time series, with observations spanning from 1917 to 2006, distributed over an area of about 85,000 km2. Trend detection analyses have been performed for monthly precipitation time series, PCI time series and monthly percentage of annual precipitation amount.

The PCI-based analysis, in particular, has provided a rapid and synthetic interpretation of the results. It has reported that, mainly for the whole area, the PCI series are affected by a negative trend, significant from about the 40 to 50 %. Negative trends in PCI would entail a more uniform distribution of the climate regime, which would be a benefit for those regions (typically the Mediterranean basin), stressed, especially during the summer season, by an increase in water demand and a reduction in available water resources. Reduction in PCI values appears diffused, with the large magnitude detected overall for the hilly areas and in particular for the Calabria region.

Coupling the PCI-based analysis with the trend detection results performed for the monthly series and monthly percentage series, it has been possible to assess that the shift towards a more uniform climate regime during the year is determined by a generalized reduction and increase in precipitation during the winter and summer months, respectively. In particular, the largest winter reductions have been detected along the

Tyrrhenian side of the southern Italy peninsula, while the summer increase appeared quite widespread over the whole investigated territory.

Acknowledgments

This study was funded by (1) the Ministry for Education, University and Research (MIUR) of Italy under the grant FARB2011 ORSA117829 and grant FARB2012 ORSA 128417; and by (2) the Project 'AQUA - Gestione sostenibile della risorsa acqua in agricoltura. Task 1.1 - Variabilità meteo-climatica ed eventi estremi di precipitazione e siccità nell'Europa Mediterranea. Decreto MIUR n. 973/2013 and Delibera CNR n. 110/2014. Department of Bio-Agrifood Science, National Research Council of Italy.

This study has also been carried out within the module TA.P05.012.004 ''Caratterizzazione di scenari nivo/pluviometrici capaci di determinare eventi di dissesto ad elevato impatto sociale ed economico'' of the Sub-Project ''Tipizzazione di eventi naturali ed antropici ad elevato impatto sociale ed economico'', as part of the Project "Rischi Naturali, Ambientali e Antropici" – Department "Scienze del Sistema Terra e Tecnologie per l'Ambiente" of the National Research Council (C.N.R.) of Italy.

References

Apaydin H, Erpul G, Bayramin I, Gabriels D (2006) Evaluation of indices for characterizing the distribution and concentration of precipitation: A case for the region of Southeastern Anatolia Project, Turkey. J Hydrol 328:726–732

Brunetti M, Buffoni L, Mangianti F, Maugeri M, Nanni T (2004) Temperature, precipitation and extreme events during the last century in Italy. Global Planet Change 40:141–149

Brunetti M, Maugeri M, Monti F, Nanni T (2006) Temperature and precipitation variability in Italy in the last two centuries from homogenised instrumental time series. Int J Climatol 26:345–381

Brunetti M, Caloiero T, Coscarelli R, Gullà G, Nanni T, Simolo C (2012) Precipitation variability and change in the Calabria region (Italy) from a high resolution daily dataset. Int J Climatol 32:55–73

Buttafuoco G, Caloiero T, Coscarelli R (2011) Spatial and temporal patterns of the mean annual precipitation at decadal time scale in southern Italy (Calabria region). Theor Appl Climatol 105:431–444

Buishand TA (1982) Some methods for testing the homogeneity of rainfall records. Journal of Hydrology, 58 11-27

Caloiero T, Coscarelli R, Ferrari E, Mancini M (2011a) Trend detection of annual and seasonal rainfall in Calabria (southern Italy). Int J Climatol 31:44–56

Caloiero T, Coscarelli R, Ferrari E, Mancini M (2011b) Precipitation change in Southern Italy linked to global scale oscillation indexes. Nat Hazards Earth Syst Sci 11:1–12

Caloiero T, Buttafuoco G, Coscarelli R, Ferrari E (2014) Spatial and temporal characterization of climate at regional scale using homogeneous monthly precipitation and air temperature data: an application in Calabria (southern Italy). Hydrol Res. published online, doi:10.2166/nh.2014.022

Cannarozzo M, Noto L, Viola F (2006) Spatial distribution of rainfall trends in Sicily (1921 2000). Phys Chem Earth 31:1201–1211

Chilès JP, Delfiner P (2012) Geostatistics: modeling spatial uncertainty, second ed. Wiley, New York

Coscarelli R, Gaudio R, Caloiero T (2004) Climatic trends: an investigation for a Calabrian basin (southern Italy). In: Proceedings of the International Symposium The basis of civilization. Water science? Rome, Italy, IAHS Publications no. 28, pp. 255–266

Coscarelli R, Caloiero T (2012) Analysis of daily and monthly rainfall concentration in Southern Italy (Calabria region). J Hydrol 416–417:145–156

De Luis M, Raventos J, Gonzalez-Hidalgo JC, Sanchez JR, Cortina J (2000) Spatial analysis of rainfall trends in the region of Valencia (East of Spain). Int J Climatol 20:1451–1469

De Luis M, Gonzalez-Hidalgo JC, Brunetti M, Longares LA (2011) Precipitation concentration changes in Spain 1946–2005. Nat Hazards Earth Syst Sci 11:1259–1265

Del Rio S, Herrero L, Fraile R, Penas AP (2011) Spatial distribution of recent rainfall trends in Spain (1961–2006). Int J Climatol 31:656–667

Diodato N (2007) Climatic fluctuations in Southern Italy since 17th century: reconstruction with precipitation records at Benevento. Climatic Change 80:411–431

Elagib NA (2011) Changing rainfall, seasonality and erosivity in the hyper-arid zone of Sudan. Land Degrad Dev 22:505–512

Feidas H, Noulopoulou Ch, Makrogiannis T, Bora-Senta E (2007) Trend analysis of precipitation time series in Greece and their relationship with circulation using surface and satellite data: 1955–2001. Theor Appl Climatol 87:155–177

Ferrari E, Caloiero T, Coscarelli R (2013) Influence of the North Atlantic Oscillation on winter rainfall in Calabria (southern Italy). Theor Appl Climatol 114:479–494

Goovaerts P (1997) Geostatistics for natural resources evaluation. Oxford University Press, New York, USA

IPCC, 2013: Summary for Policymakers. In: Climate Change 2013: The Physical Science Basis. Contribution of Working Group I to the Fifth Assessment Report of the Intergovernmental Panel on Climate Change [Stocker,T.F., D. Qin, G.-K. Plattner, M. Tignor, S. K. Allen, J. Boschung, A. Nauels, Y. Xia, V. Bex and P.M. Midgley (eds.)]. Cambridge University Press, Cambridge, United Kingdom and New York, NY, USA

Kendall MG (1962) Rank Correlation Methods. Hafner Publishing Company, New York

Journel AG, Huijbregts CJ (1978) Mining Geostatistics. Academic Press, New York

Lionello P, Giorgi F (2007) Winter precipitation and cyclones in the Mediterranean region: future climate scenarios in a regional simulation. Adv Geosci 12:153–158

Longobardi A, Villani P (2010) Trend analysis of annual and seasonal rainfall time series in the Mediterranean area. Int J Climatol 30:1538–1546

Longobardi A, Meddi H, Meddi M, Mehaiguene M (2011) Characterization of precipitation variability in the Mediterranean basin. In: Proceedings VI International

Workshop EWRA 2011 Water Engineering and Management in a Changing Environment. Catania, Italy, Quaderni CSEI Catania, III series, no. 6, pp. 22–32.

Mann HB (1945) Nonparametric tests against trend. Econometrica 13:245–259

Martins DS, Raziei T, Paulo AA, Pereira LS (2012) Spatial and temporal variability of precipitation drought in Portugal. Nat Hazard Earth Sys Sci 12:1493–1501

Mehta AV, Yang S (2008) Precipitation climatology over Mediterranean Basin from en years of TRMM measurements. Adv Geosci 17:87–91

Michiels P, Gabriels D, Hartman R (1992) Using the seasonal and temporal precipitation concentration index for characterizing the monthly rainfall distribution in Spain. Catena 19:43–58

Ngongondo C, Xu CY, Gottshalk L, Alemaw B (2011) Evaluation of spatial and temporal characteristics of rainfall in Malawi: a case of data scares region. Theor Appl Climatol 106:79–93

Nsubuga FNW, Olwoch JM, deW Rautenbach CJ, Botai OJ (2014) Analysis of mid-twentieth century rainfall trends and variability over southwestern Uganda. Theor Appl Climatol 115:53–71

Oliver JE (1980) Monthly precipitation distribution: a comparative index. The Professional Geographer 32:300–309

Palmieri S, Siani AM, D'Agostino A (1991) Climate fluctuations and trends in Italy within the last hundred years. Ann Geophys 9:769–776

Peterson TC, Easterling DR, Karl TR, Groisman P, Nicholls N, Plummer N, Torok S, Auer I, Boehm R, Gullett D, Vincent L, Heino R, Tuomenvirta H, Mestre O, Szentimrey T, Salinger J, Forland EJ, Hanssenbauer I, Alexandersson H, Jones P, Parker D (1998) Homogeneity adjustments of in situ atmospheric climate data: a review. Int J Climatol 18:1493–1517

Piccarreta M, Capolongo D, Boenzi F (2004) Trend analysis of precipitation and drought in Basilicata from 1923 to 2000 within a Southern Italy context. Int J Climatol 24:907–922.

Piccarreta M, Pasini A, Capolongo D, Lazzari M (2013) Changes in daily precipitation extremes in the Mediterranean from 1951 to 2010: the Basilicata region, southern Italy. Int J Climatol 33:3229–3248

Raziei T, Bordi I, Pereira LS (2008) A precipitation-based regionalization for Western Iran and regional drought variability. Hydrol Earth Syst Sc 12:1309-1321

Reale M, Lionello P (2013) Synoptic climatology of winter intense precipitation events along the Mediterranean coasts. Nat Hazards Earth Syst Sci 13:1707–1722

Sen PK (1968) Estimates of the regression coefficient based on Kendall's tau J Amer Statist Assoc 63, 1379–1389.

Shi P, Qiao X, Chen X, Zhou M, Qu S, Ma X, Zhang Z (2014) Spatial distribution and temporal trends in daily and monthly precipitation concentration indices in the upper reaches of the Huai River, China. Stoch Environ Res Risk Assess 28, 201–212

Singh N, Krishna Kumar K, Soman MK (1989) Some features of the periods contributing specified percentages of rainfall to annual total in Kerala, India. Theor Appl Climatol 39:160–170

Sirangelo B, Caloiero T, Coscarelli R, Ferrari E (2014) A stochastic model for the analysis of the temporal change of dry spells. Stoch Environ Res Risk Assess, published online, DOI 10.1007/s00477-014-0904-5.

Wackernagel H (2003) Multivariate Geostatistics: an introduction with applications. Springer-Verlag: Berlin

Webster R, Oliver MA (2007) Geostatistics for Environmental Scientists. Wiley, Chichester, UK

Xoplaki E, Luterbacher J, González-Rouco JF (2006) Mediterranean summer temperature and winter precipitation, large-scale dynamics, trends. Nuovo Cimento C 29:45–54

Xu L, Zhou H, Liang C, Du L, Li H (2010) Spatial and temporal variability of annual and seasonal precipitation over the desert region of China during 1951-2005. Hydrol Process 24:2947–2959

Figures captions

Fig. 1. The study area with the localization of the 559 rain gauges.

Fig. 2. The mean annual precipitation map of the study area and the distribution of the mean monthly precipitation proportional coefficients.

Fig. 3. Trend of the monthly precipitation expressed as % of rain gauges of the whole data set.

Fig. 4. Distribution, for each month, of the precipitation trend.

Fig. 5. Distribution of the PCI values and variogram of the PCI (in the box).

Fig. 6. Distribution of the PCI trend and summary of the results (in the box) for different Significant Levels.

Fig. 7. Distribution of the CV-PCI values and variogram of the CV-PCI (in the box).

Fig. 8. Distribution of the CV-PCI trend and summary of the results (in the box) for different Significant Levels.

Fig. 9. Trend of the percentage of the monthly precipitation contribution with respect to the total annual, expressed as % of rain gauges of the whole data set.

Fig. 10. Trend distribution, for each month, of the percentage of the monthly precipitation contribution with respect to the total annual.

Fig. 11. Results of the MK trend analysis (SL = 0.10) applied to the percentages of the monthly precipitation contributions with respect to the total annual, expressed as % of rain gauges for: a Basilicata, b Calabria, c Campania, d Apulia, e Sicily regions and f the whole study area.

Fig. 12. Results of the MK trend analysis (SL = 0.05) applied to the percentages of the monthly precipitation contributions with respect to the total annual, expressed as % of rain gauges for: a Basilicata, b Calabria, c Campania, d Apulia, e Sicily regions and f the whole study area.

Fig. 13. Results of the MK trend analysis (SL = 0.01) applied to the percentages of the monthly precipitation contributions with respect to the total annual, expressed as % of rain gauges for: a Basilicata, b Calabria, c Campania, d Apulia, e Sicily regions and f the whole study area.

Fig. 14. Spatial distribution, for each month, of the MK trend sign and with different SL values evaluated for the percentages of the monthly precipitation contributions with respect to the total annual.

Figure 1
Click here to download Figure: Fig.1.tif

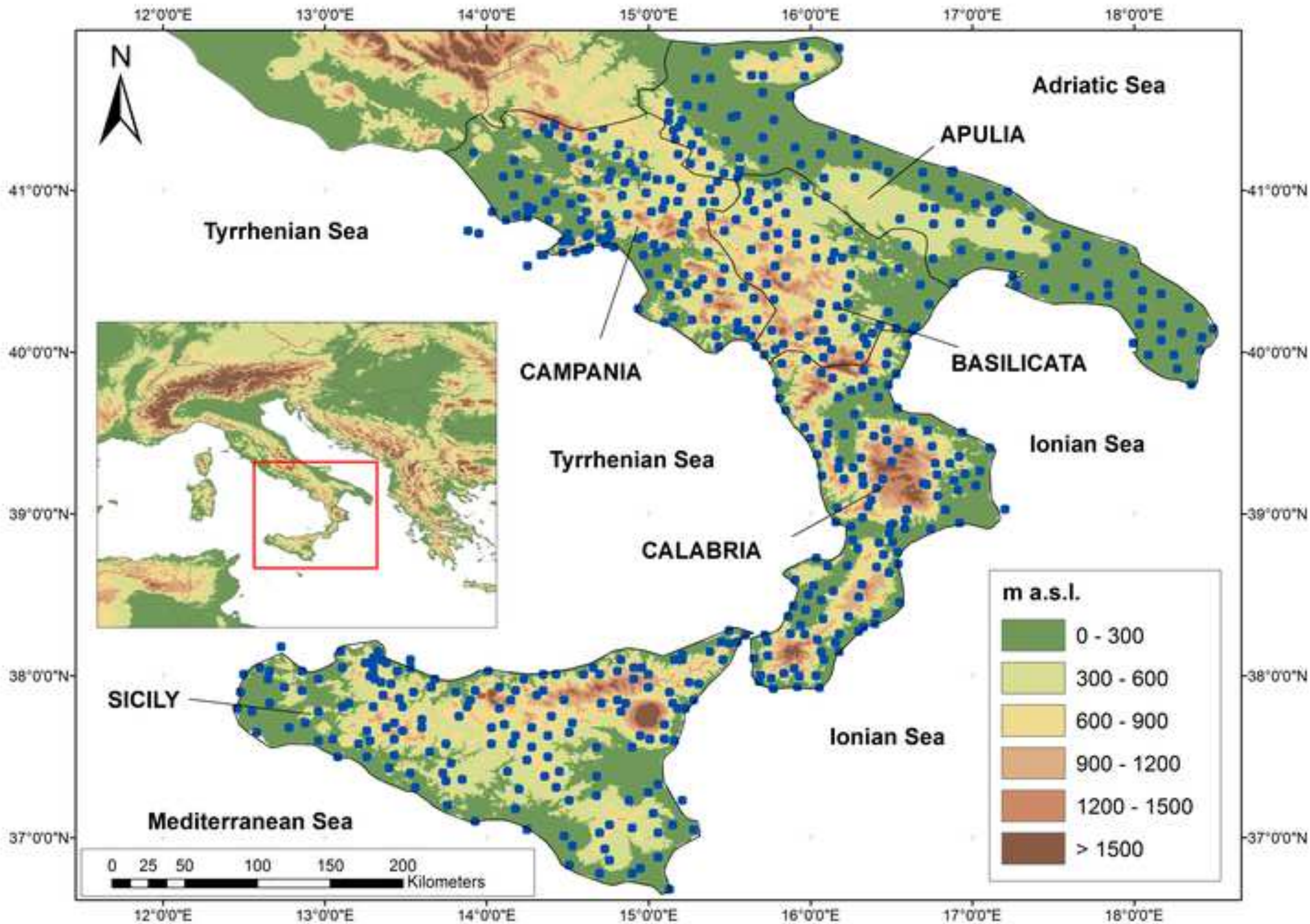

Figure 2
Click here to download Figure: Fig.2.tif

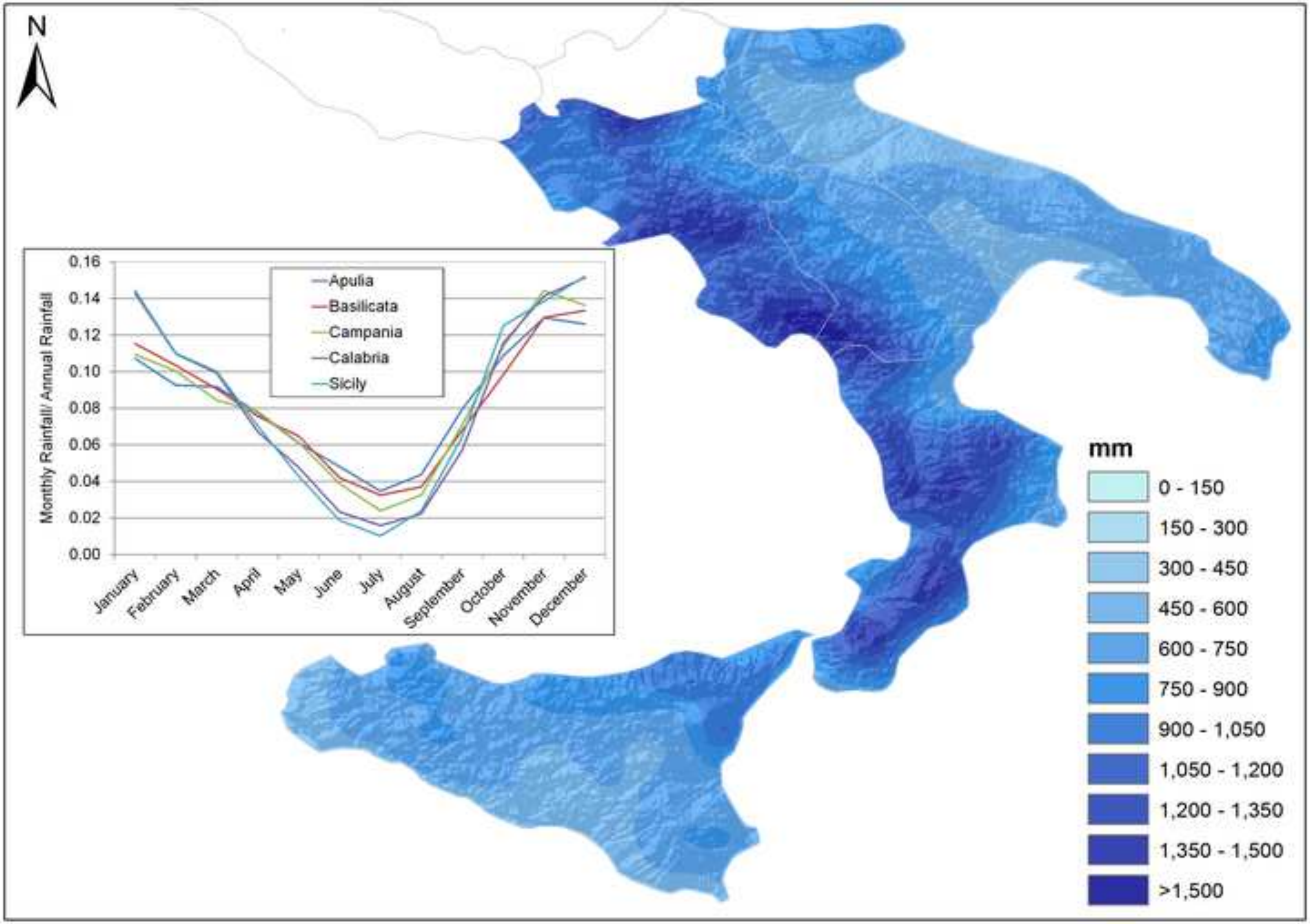

Figure 3
Click here to download Figure: Fig.3.tif

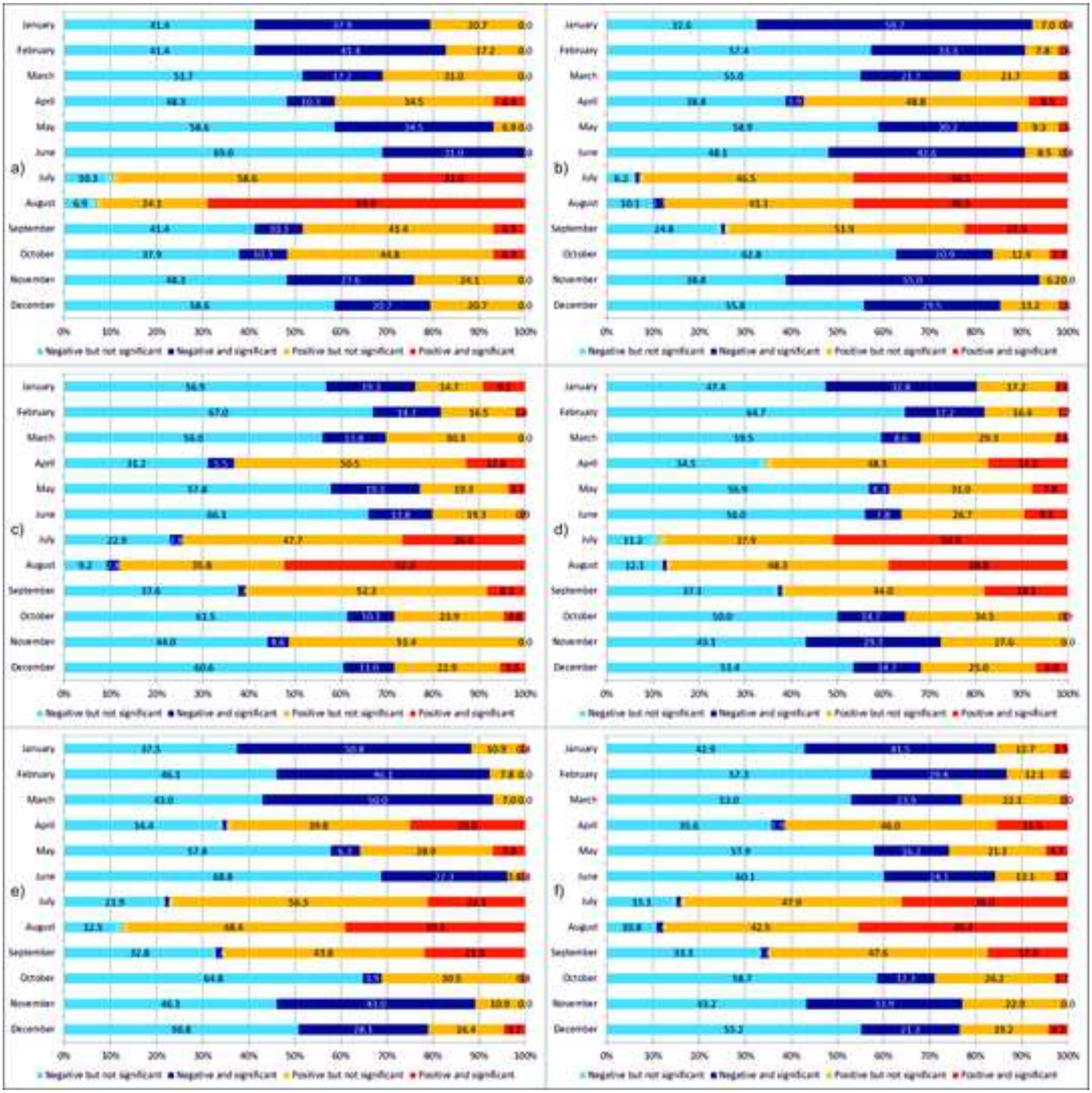

Figure 4

Click here to download Figure: Fig.4.tif

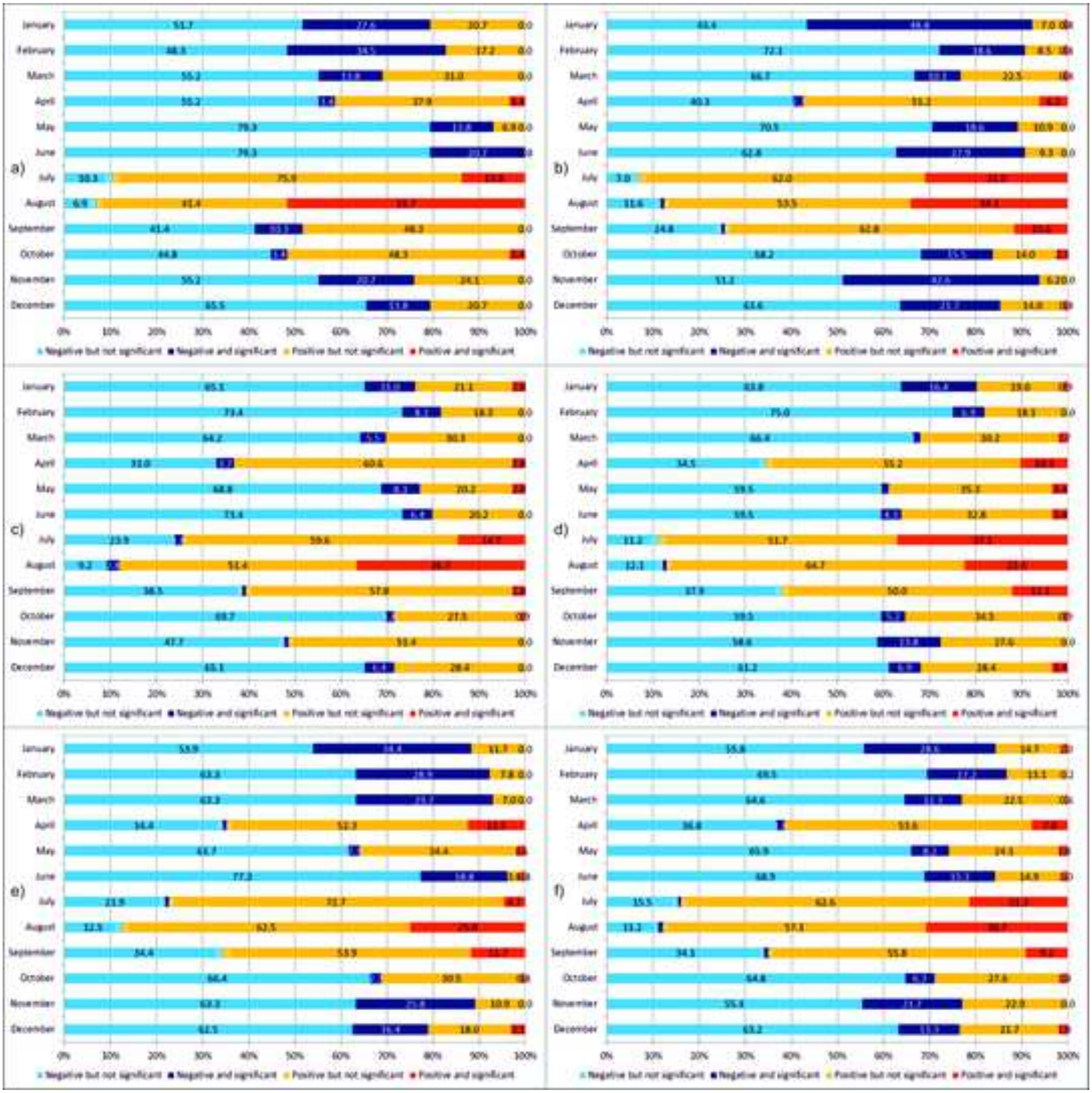

Figure 5
Click here to download Figure: Fig.5.tif

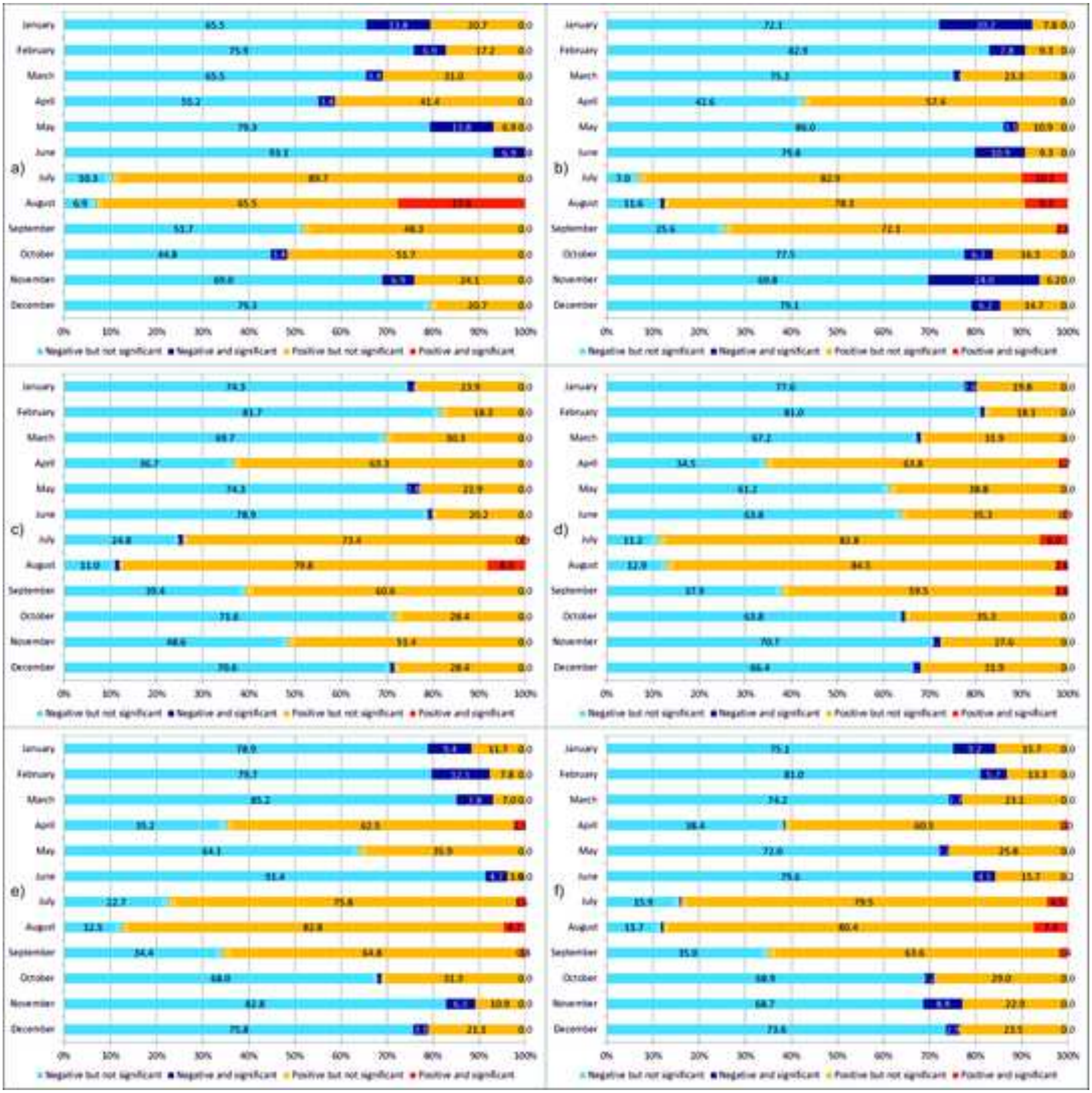

Figure 6
Click here to download Figure: Fig.6.tif

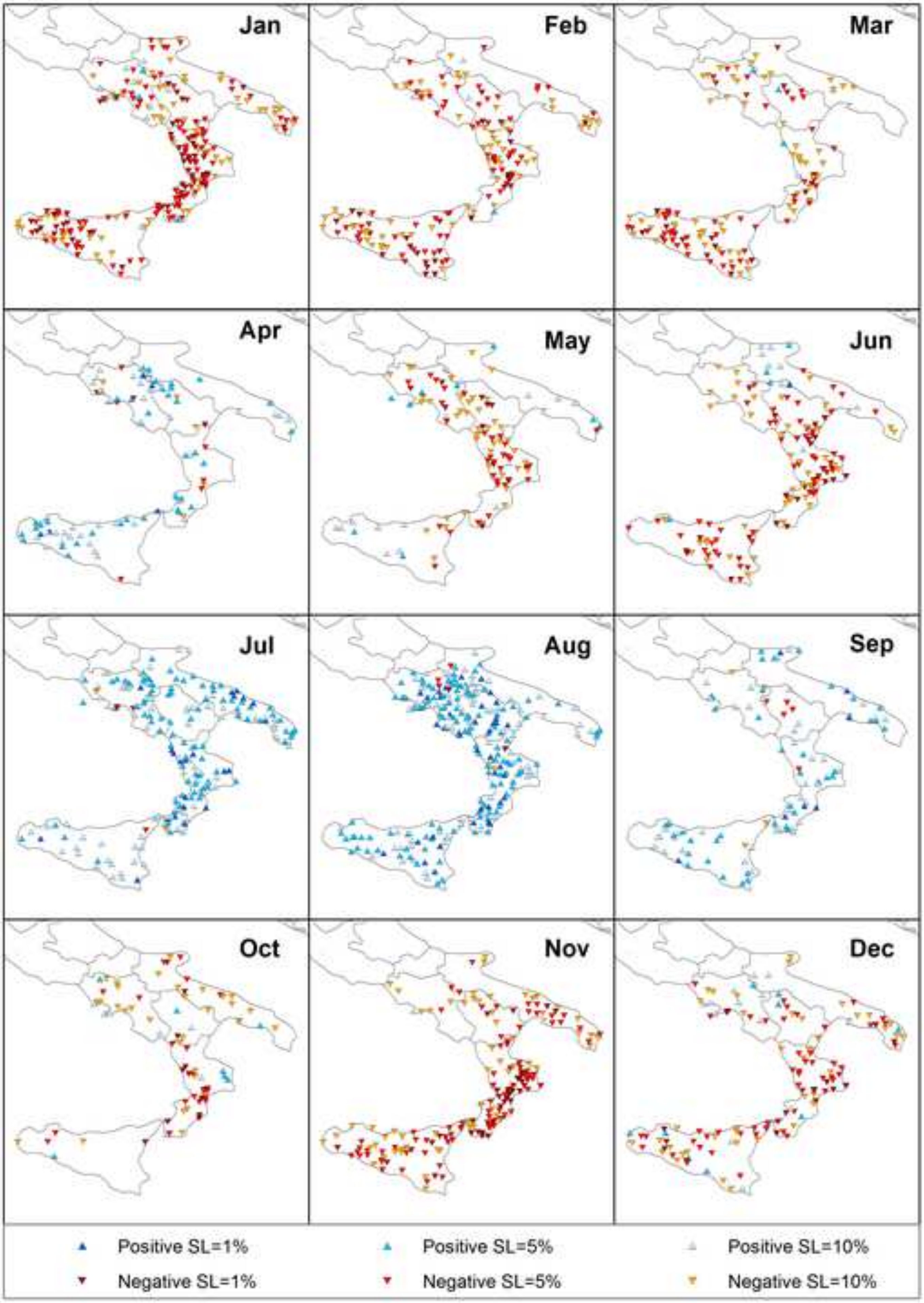

Figure 7

Click here to download Figure: Fig.7.tif

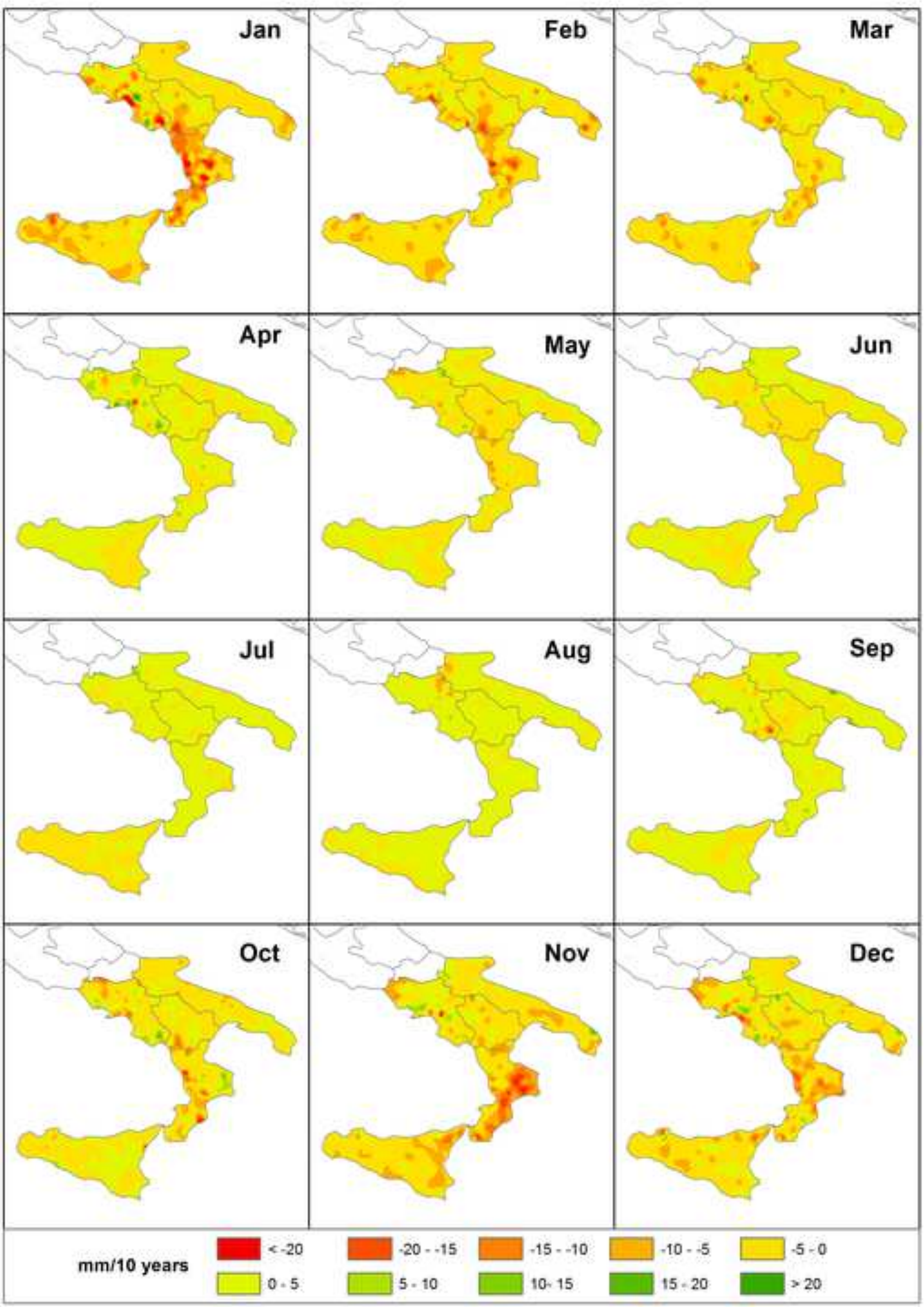

Figure 8

Click here to download Figure: Fig.8.tif

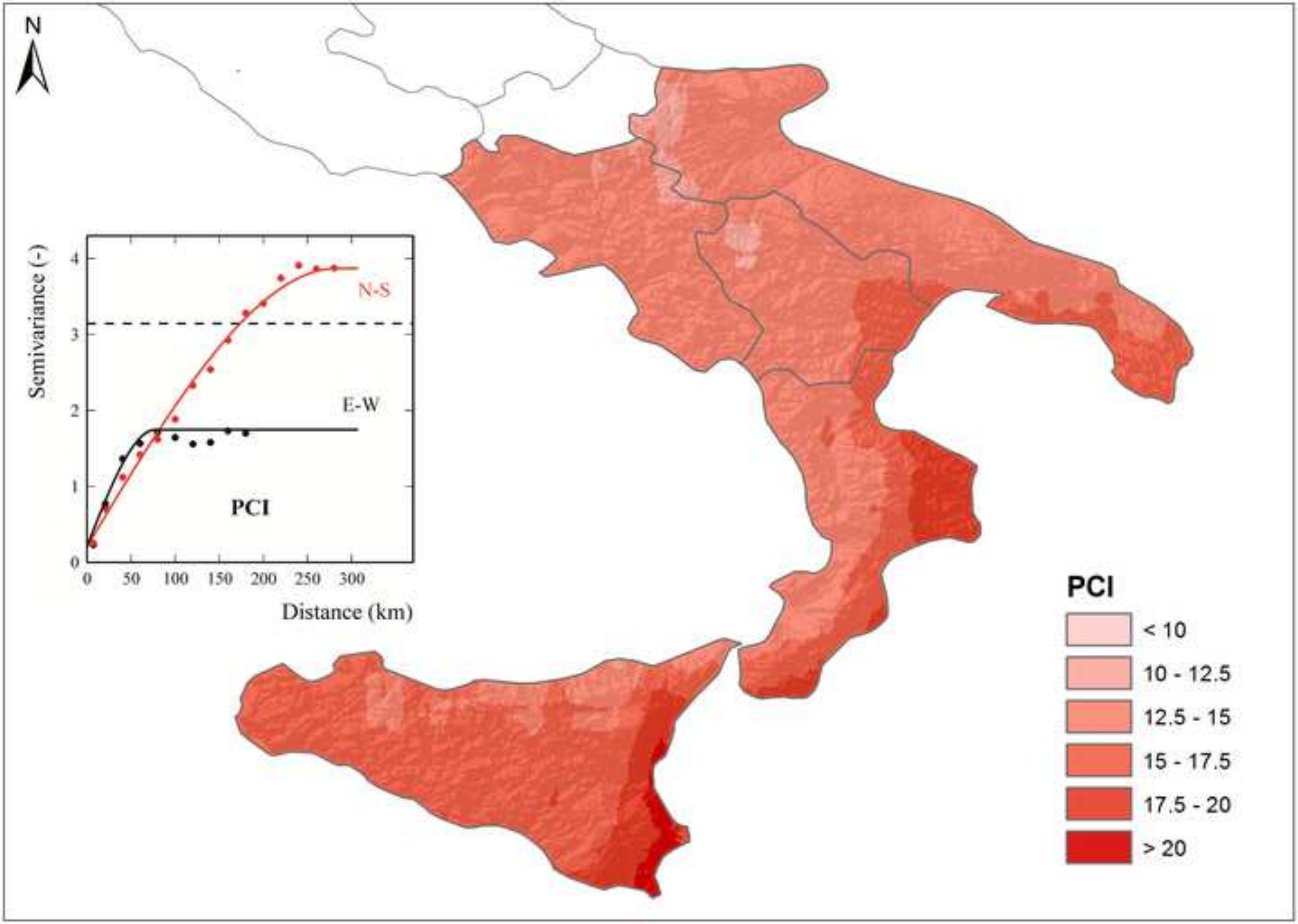

Figure 9

Click here to download Figure: Fig.9.tif

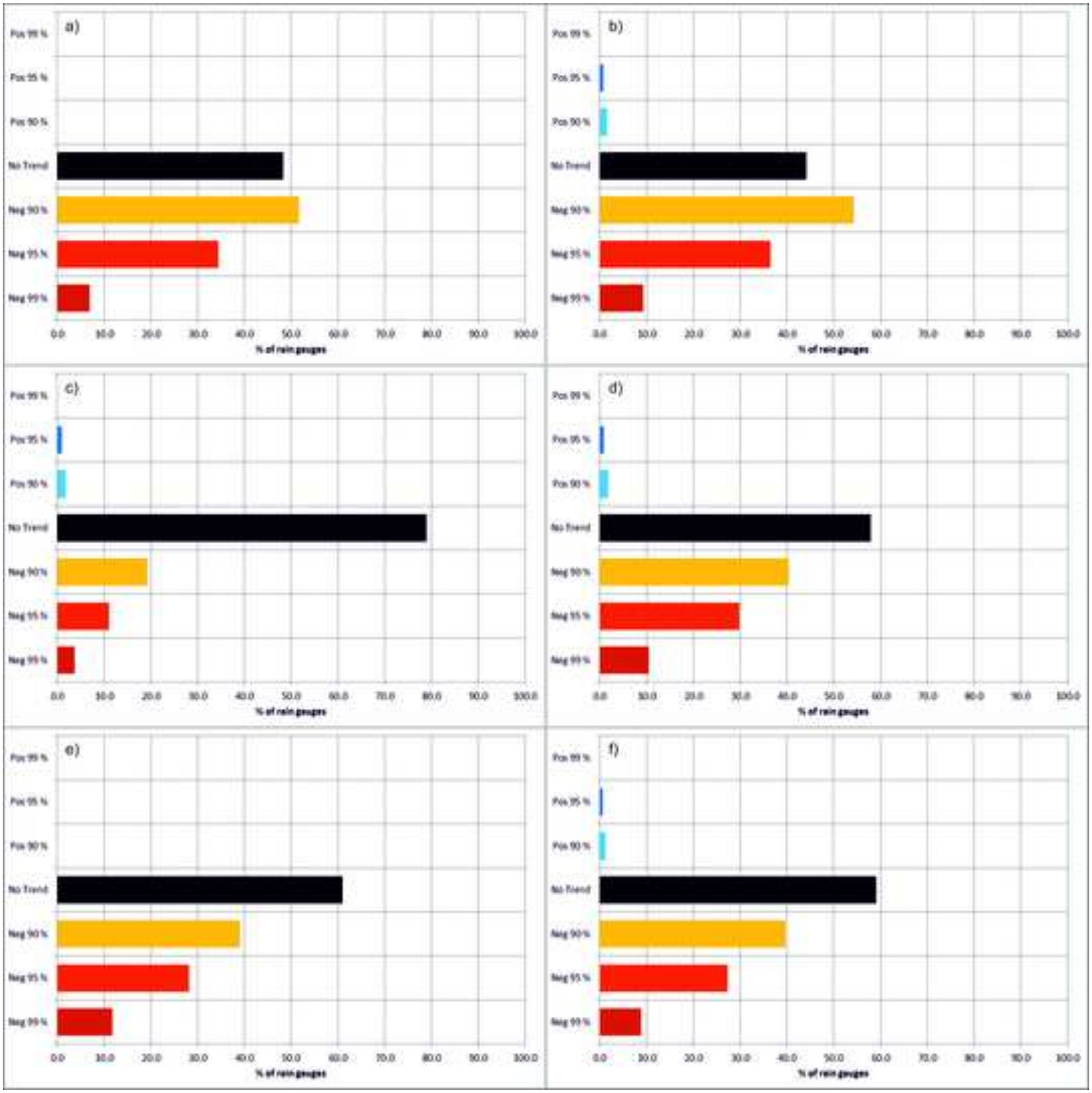

Figure 10
Click here to download Figure: Fig.10.tif

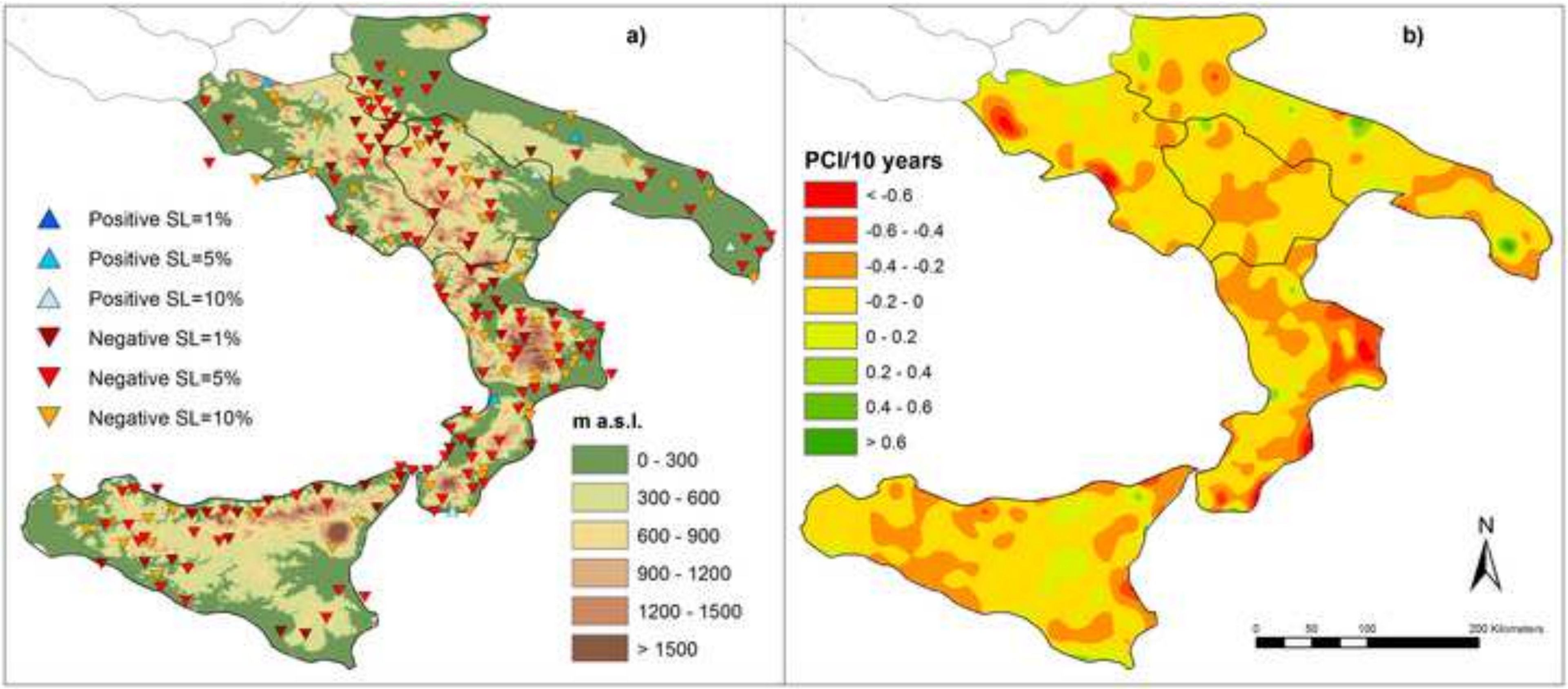

Figure 11
Click here to download Figure: Fig.11.tif

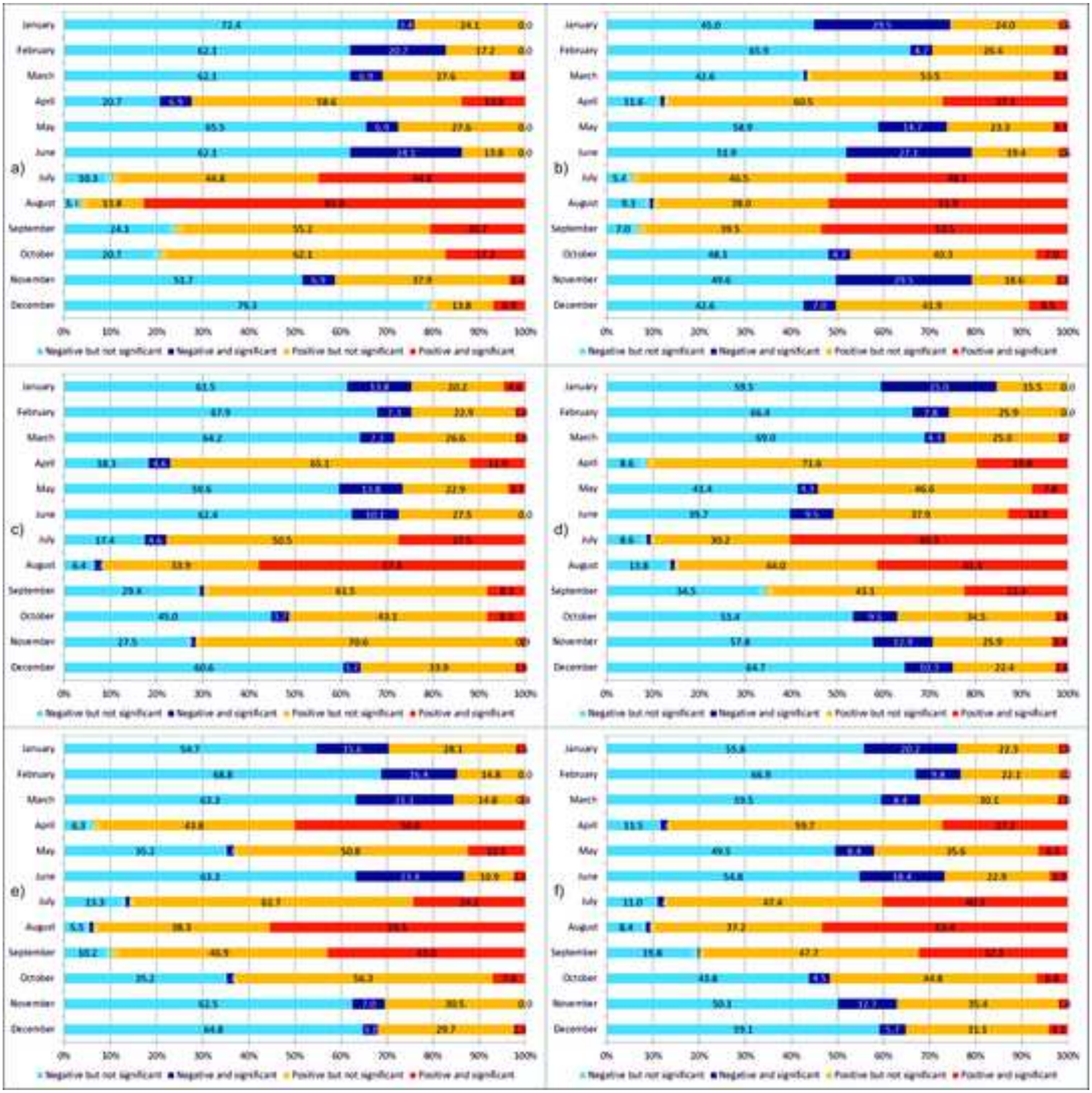

Figure 12
Click here to download Figure: Fig.12.tif

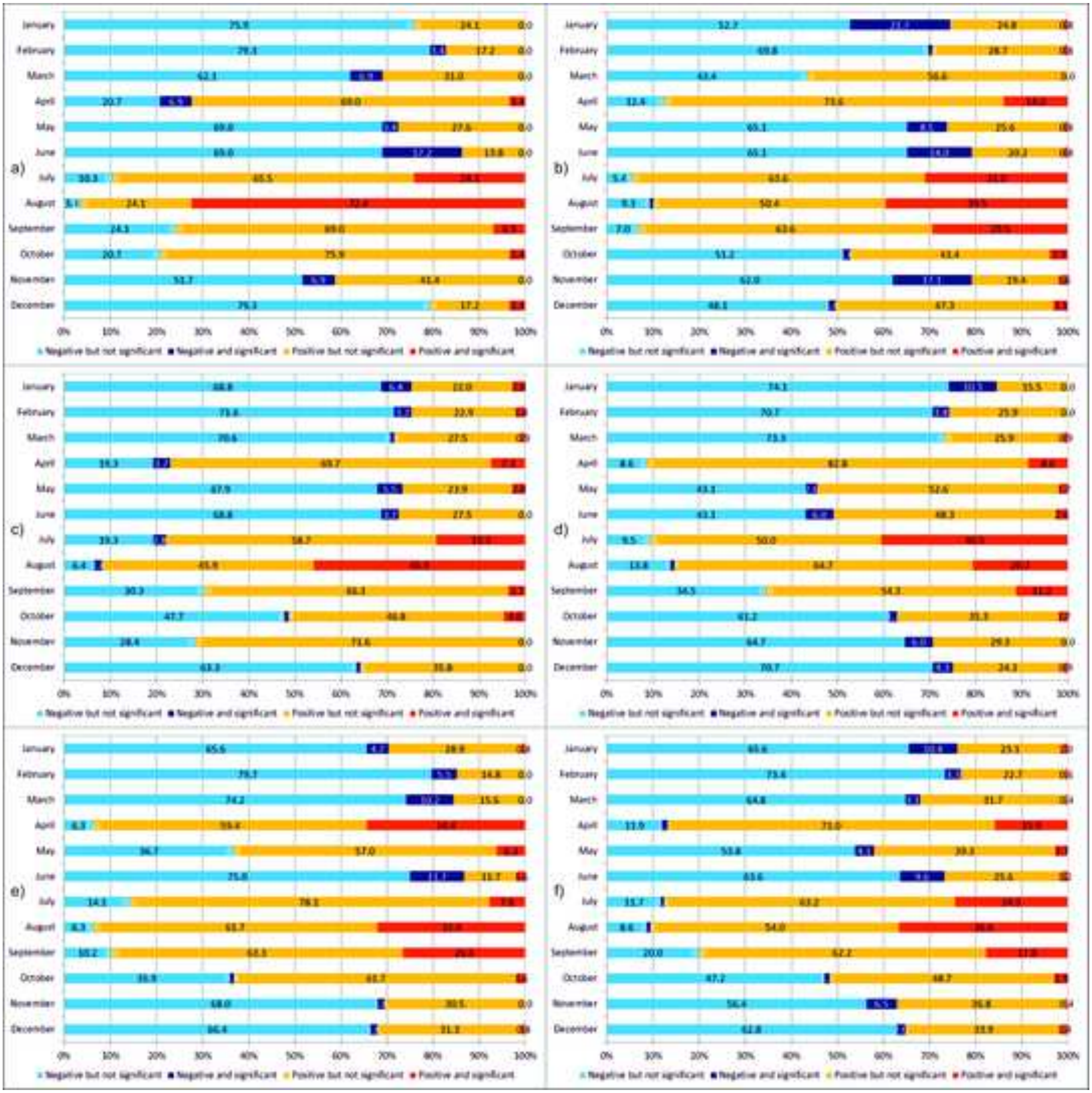

Figure 13
Click here to download Figure: Fig.13.tif

Figure 14
Click here to download Figure: Fig.14.tif

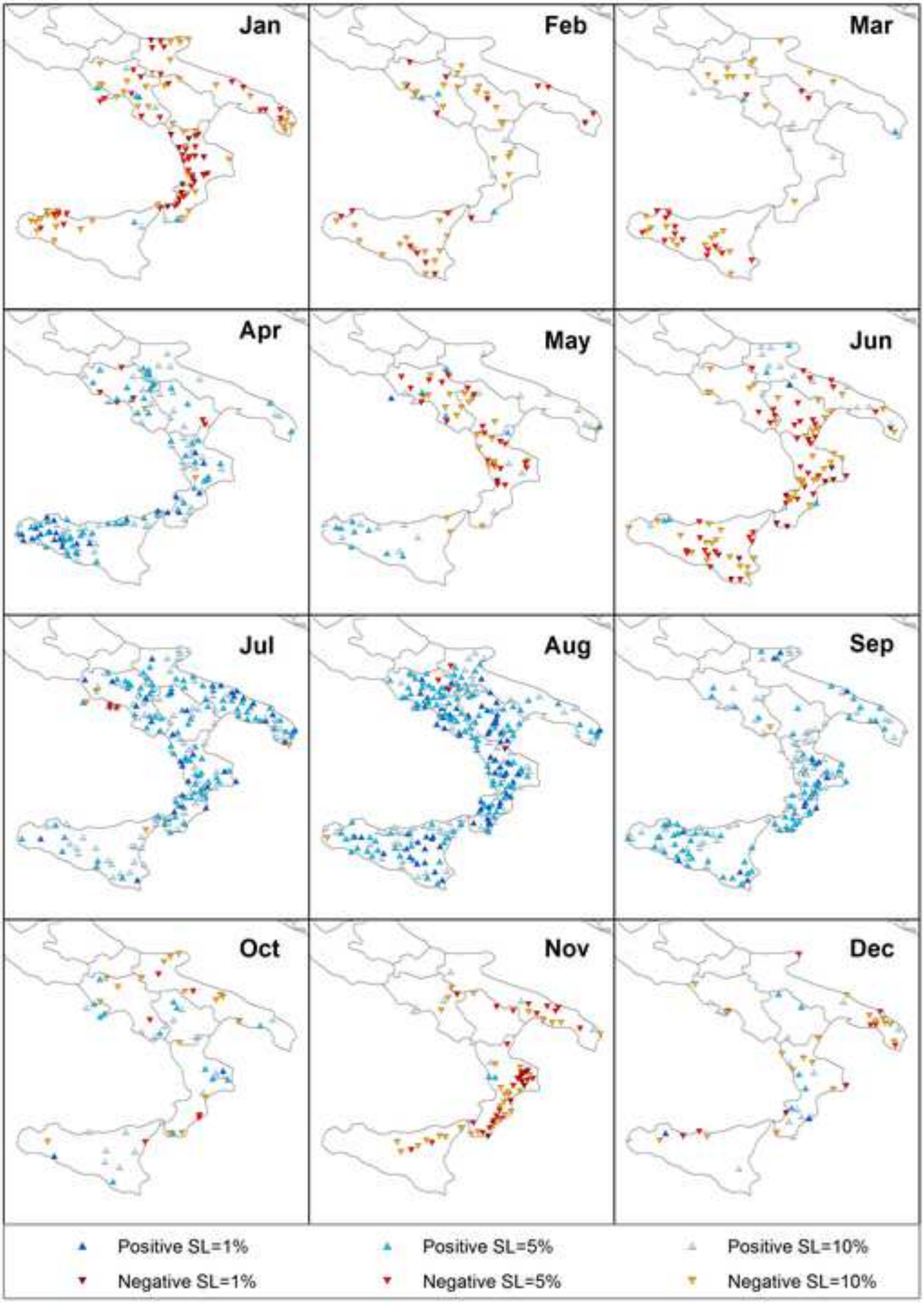

Table 1. Variogram model parameters for PCI at annual scale.

Variable	Direction	Model	Sill	Range (km)
	-	Nugget	0.2089	-
PCI	N-S	Spherical	3.6608	284.77
	E-W	Spherical	1.5382	77.23